EFT APPROACHES FOR HIGGS IN e-p COLLISIONS

Mukesh Kumar

NITHEP, MITP & School of Physics,
University of the Witwatersrand
Johannesburg, South Africa.

LHeC and FCC-eh Workshop
11-13 September 2017
CERN

On behalf of LHeC and FCC-he Higgs-Top group

OUTLINE

0. • Baseline for future e-p machine

I. • Overview of single Higgs production

II. • Double Higgs production

III. • Higher Order λ correction to hVV

IV. • CP-even neutral Higgs in two-Higgs doublet model

V. • Summary and Discussions

LHeC/FCC-he

A Baseline for the FCC-he

Oliver Brüning[1] Max Klein[1,2], Daniel Schulte[1], Frank Zimmermann[1]
[1] CERN, [2] University of Liverpool
March 3rd, 2016

Table 1: Baseline parameters of future electron-proton collider configurations based on the ERL electron linac.

parameter [unit]	LHeC CDR	ep at HL-LHC	ep at HE-LHC	FCC-he
E_p [TeV]	7	7	15	50
E_e [GeV]	60	60	60	60
$\sqrt{s}$ [TeV]	1.3	1.3	1.9	3.5
bunch spacing [ns]	25	25	25	25
protons per bunch [10^{11}]	1.7	2.2	2.2	1
ϵ_p [μm]	3.7	2	2	2.2
electrons per bunch [10^9]	1	2.3	2.3	2.3
electron current [mA]	6.4	15	15	15
IP beta function β_p^* [cm]	10	7	10	15
hourglass factor	0.9	0.9	0.9	0.9
pinch factor	1.3	1.3	1.3	1.3
luminosity [10^{33}cm^{-2}s^{-1}]	1.3	10.1	15.1	9.2

Higgs production modes

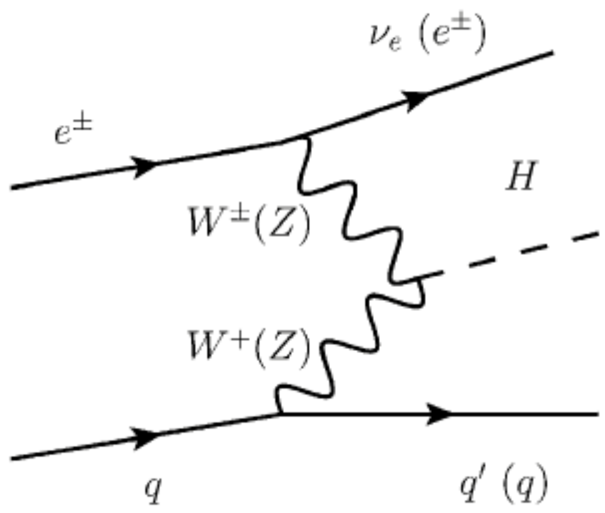

FIG. 1. Leading order diagram for the production of a standard model Higgs boson in ep collisions for the charged current and neutral current processes.

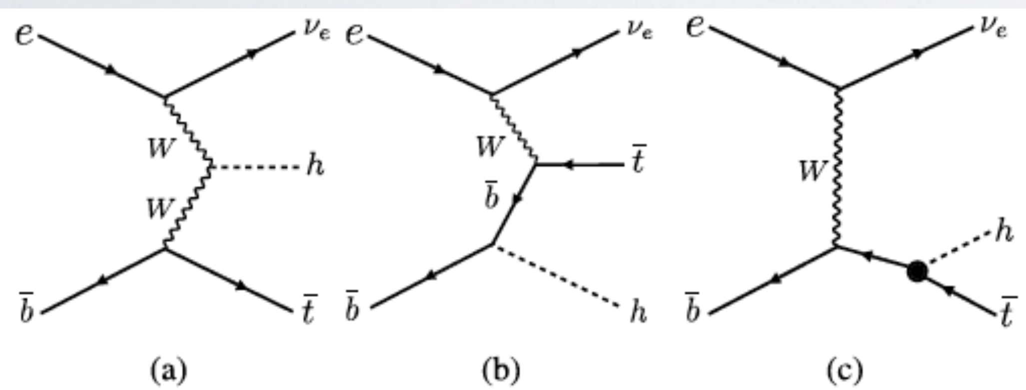

Fig. 1. Leading order Feynman diagrams contributing to the process $pe^- \to \bar{t}\, h\, \nu_e$ at the LHeC. The black dot in the Feynman diagram (c) denotes the top-Higgs coupling which is the subject of this study.

I'll talk about this in top-session

Measuring Higgs-self coupling

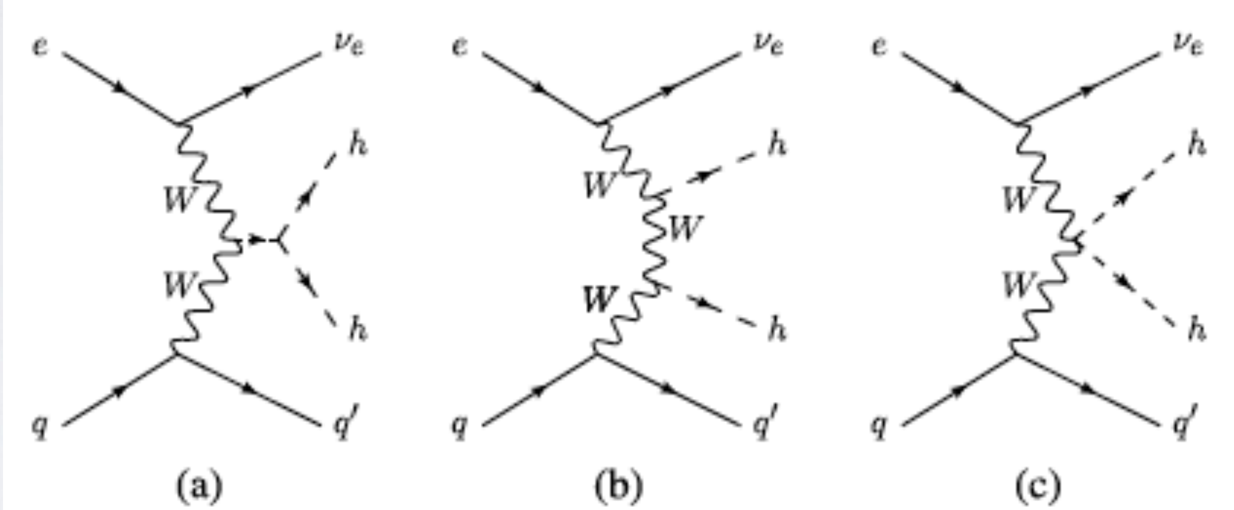

Fig. 1. Leading order diagrams contributing to the process $pe^- \to hhj\nu_e$ with $q \equiv u, c, \bar{d}, \bar{s}$ and $q' \equiv d, s, \bar{u}, \bar{c}$ respectively.

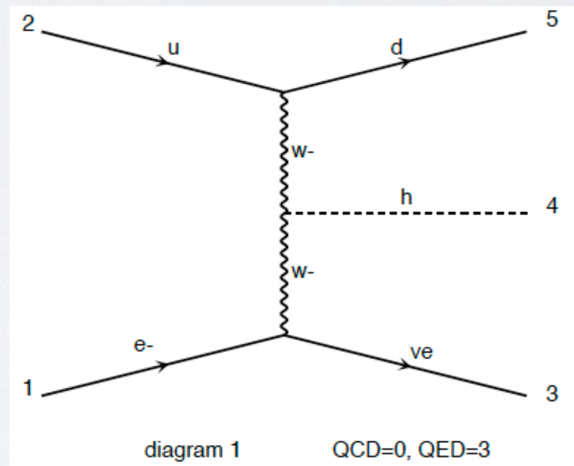

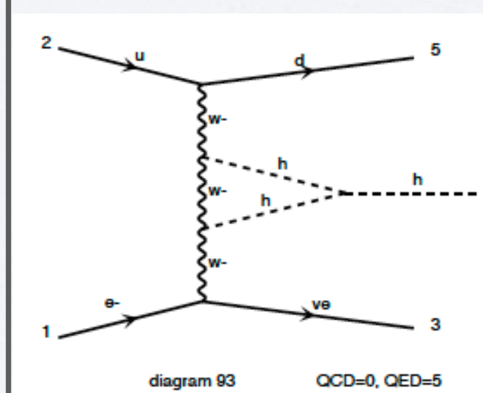

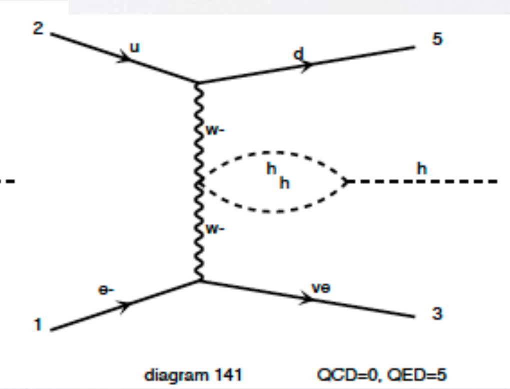

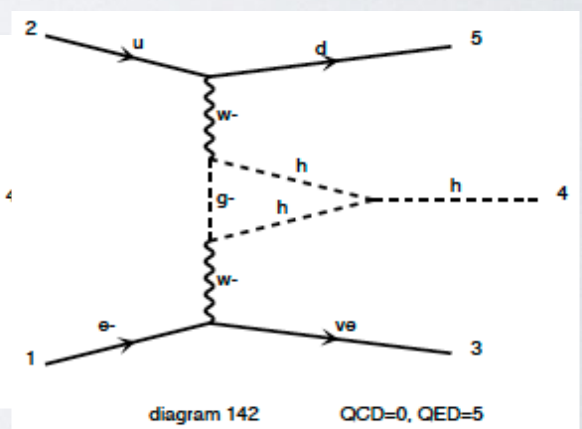

I.

PHYSICAL REVIEW D 82, 016009 (2010)

Higgs boson searches and the $Hb\bar{b}$ coupling at the LHeC

Tao Han* and Bruce Mellado†
Department of Physics, University of Wisconsin, Madison, Wisconsin 53706, USA
(Received 15 September 2009; published 30 July 2010)

Once the existence of the Higgs boson is established at the CERN Large Hadron Collider (LHC), the focus will be shifted toward understanding its couplings to other particles. A crucial aspect is the measurement of the bottom Yukawa coupling, which is challenging at the LHC. In this paper we study the use of forward jet tagging as a means to secure the observation and to significantly improve the purity of the Higgs boson signal in the $H \to b\bar{b}$ decay mode from deep inelastic electron-proton scattering at the LHC. We demonstrate that the requirement of forward jet tagging in charged current events strongly enhances the signal-to-background ratio. The impact of a veto on additional partons is also discussed. Excellent response to hadronic shower and b-tagging capabilities are pivotal detector performance aspects.

DOI: 10.1103/PhysRevD.82.016009 PACS numbers: 11.15.Ex, 14.80.Bn

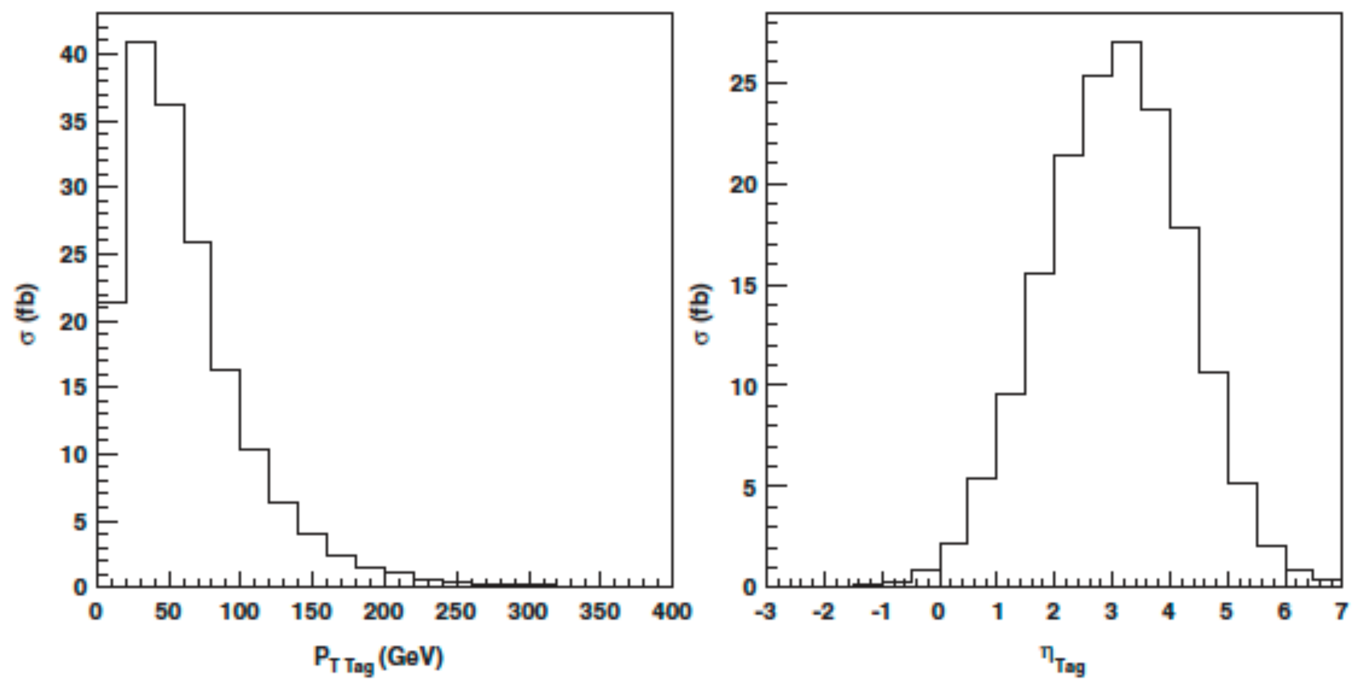

consider the physics potential for the proposed proton-electron collider, the LHeC. We studied the use of forward jet tagging as a means to secure the observation of the Higgs boson in the $H \to b\bar{b}$ decay mode, and to significantly improve the purity of the signal. An excellent signal-to-background ratio of almost a factor of 5 can be achieved for the CC process while allowing for a significant rate of Higgs boson events. With this we believe that a measurement of the bottom Yukawa coupling at the LHeC may be feasible by means of combining the knowledge from the LHC on $H \to WW^\star, \tau\tau$.

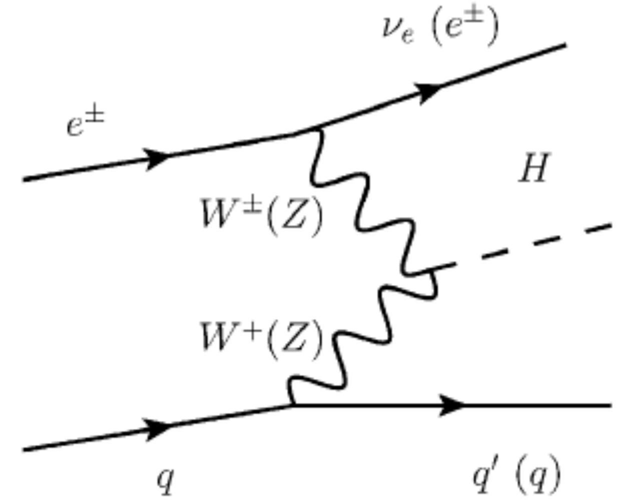

FIG. 1. Leading order diagram for the production of a standard model Higgs boson in ep collisions for the charged current and neutral current processes.

$$\sigma(fa \to f'X) \approx \int dx dp_T^2 P_{V/f}(x, p_T^2)\sigma(Va \to X)$$

$$P^T_{V/f}(x, p_T^2) = \frac{g_V^2 + g_A^2}{8\pi^2}\frac{1+(1-x)^2}{x}\frac{p_T^2}{(p_T^2+(1-x)M_V^2)^2} \tag{4}$$

$$P^L_{V/f}(x, p_T^2) = \frac{g_V^2 + g_A^2}{4\pi^2}\frac{1-x}{x}\frac{(1-x)M_V^2}{(p_T^2+(1-x)M_V^2)^2}. \tag{5}$$

These expressions lead us to the following observations:

(1) Unlike the QCD partons that scale like $1/p_T^2$ at the low transverse momentum, the final state quark f' typically has $p_T \sim \sqrt{1-x}M_V \le M_W$.

(2) Because of the $1/x$ behavior for the gauge boson distribution, the outgoing parton energy $(1-x)E$ tends to be high. Consequently, it leads to an energetic forward jet with small, but finite, angle with respect to the beam.

(3) At high p_T, $P^T_{V/f} \sim 1/p_T^2$ and $P^L_{V/f} \sim 1/p_T^4$, and thus the contribution from the longitudinally polarized gauge bosons is relatively suppressed at high p_T to that of the transversely polarized.

I.

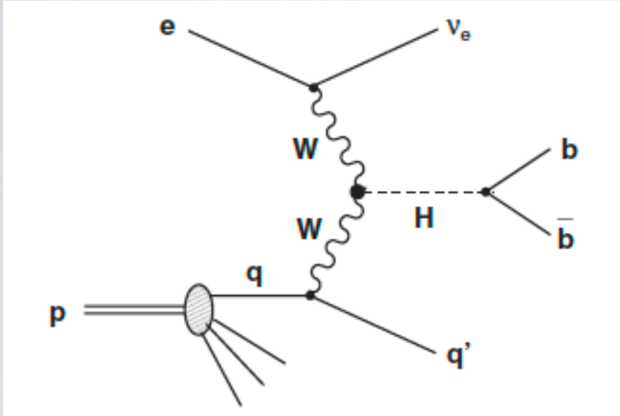

PRL 109, 261801 (2012) PHYSICAL REVIEW LETTERS

Azimuthal Angle Probe of Anomalous HWW Couplings at a High Energy ep Collider

Sudhansu S. Biswal,[1] Rohini M. Godbole,[2] Bruce Mellado,[3,4] and Sreerup Raychaudhuri[5]

$$\mathcal{L}_{\rm int} = -gM_W\left(W_\mu W^\mu + \frac{1}{2\cos\theta_W} Z_\mu Z^\mu\right)H.$$

$$e^-(k_1) + q(k_2) \to \nu_e(p_1) + q'(p_2) + H(p_3)$$

$$\Gamma^{\rm BSM}_{\mu\nu}(p,q) = \frac{g}{M_W}[\lambda(p\cdot q g_{\mu\nu} - p_\nu q_\mu) + i\lambda' \epsilon_{\mu\nu\rho\sigma} p^\rho q^\sigma],$$

criteria may be summarized as follows: (1) It is required that $MET > 25$ GeV. (2) Two b partons with $p_T^b > 30$ GeV and $|\eta_b| < 2.5$ must be present. The invariant mass of these b partons must lie within 10 GeV of the Higgs boson mass. (3) Of the remaining partons, the leading one must have $p_T > 30$ GeV and $1 < \eta < 5$. This will be called the forward tagging parton. (4) We require $\Delta\varphi_{{\rm MET}-J} > 0.2$ rad for all the jets (J). (5) A veto on leptons ($\ell = e, \mu, \tau$) with $p_T^\ell > 10$ GeV and $|\eta_\ell| < 2.5$ is required. (6) The invariant mass of the Higgs boson candidate and the forward tagging jet must be greater than 250 GeV. (7) We require a b-tagging efficiency $\varepsilon_b = 0.6$ for $|\eta_b| < 2.5$. The mistagging factors for c and light quark jets are taken as 0.1 and 0.01, respectively.

$$\overline{|\mathcal{M}|^2} = \left(\frac{4\pi^3\alpha^3}{\sin^6\theta_W}\right)\frac{1}{M_W^2(\hat{t}_1 - M_W^2)^2(\hat{u}_2 - M_W^2)^2} \times [4M_W^4\hat{s}\hat{s}_1 + \lambda^2\{\hat{t}_1\hat{u}_2(\hat{s}^2 + \hat{s}_1^2 + \hat{t}_1\hat{u}_2 - 2\hat{t}_2\hat{u}_1) + (\hat{s}\hat{s}_1 - \hat{t}_2\hat{u}_1)^2\} + 2\lambda M_W^2(\hat{s} + \hat{s}_1)(\hat{s}\hat{s}_1 + \hat{t}_1\hat{u}_2 - \hat{t}_2\hat{u}_1) + \lambda'^2\{\hat{t}_1\hat{u}_2(\hat{s}^2 + \hat{s}_1^2 - \hat{t}_1\hat{u}_2 + 2\hat{t}_2\hat{u}_1) - (\hat{s}\hat{s}_1 - \hat{t}_2\hat{u}_1)^2\} - 2\lambda' M_W^2(\hat{s} - \hat{s}_1)(\hat{s}\hat{s}_1 + \hat{t}_1\hat{u}_2 - \hat{t}_2\hat{u}_1) + 2\lambda\lambda'\hat{t}_1\hat{u}_2(\hat{s}_1^2 - \hat{s}^2)],$$

$$\mathcal{M}_\lambda \propto +\lambda \vec{p}_{T1}.\vec{p}_{T2}, \qquad \mathcal{M}'_\lambda \propto -\lambda' \vec{p}_{T1}.\vec{p}_{T2},$$

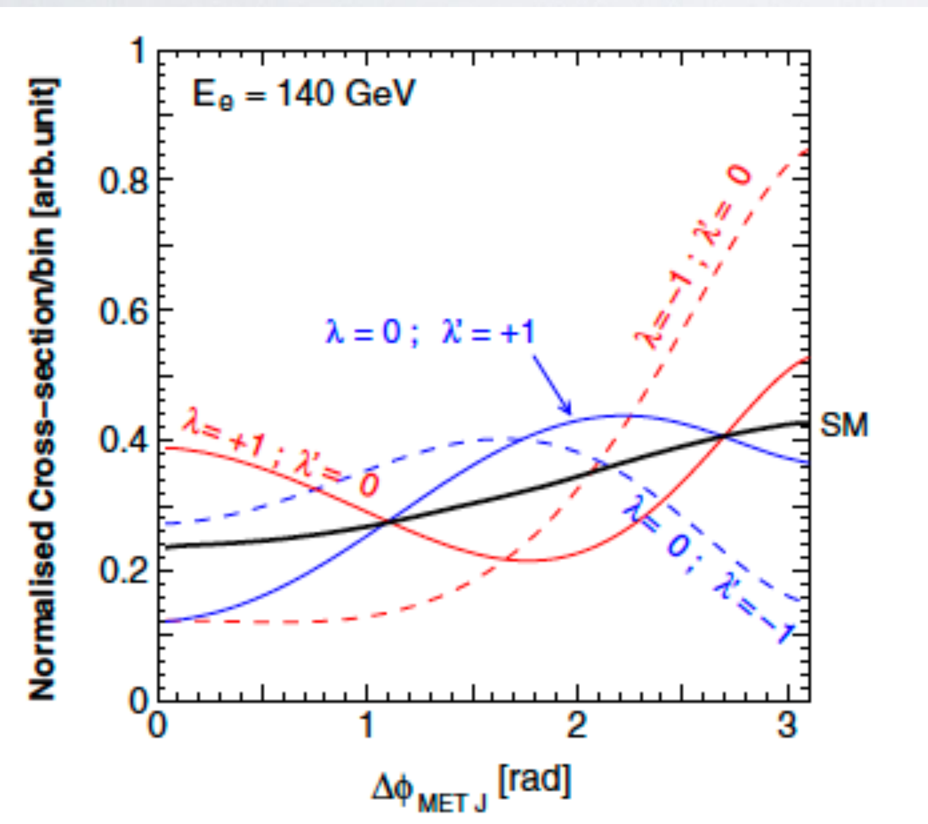

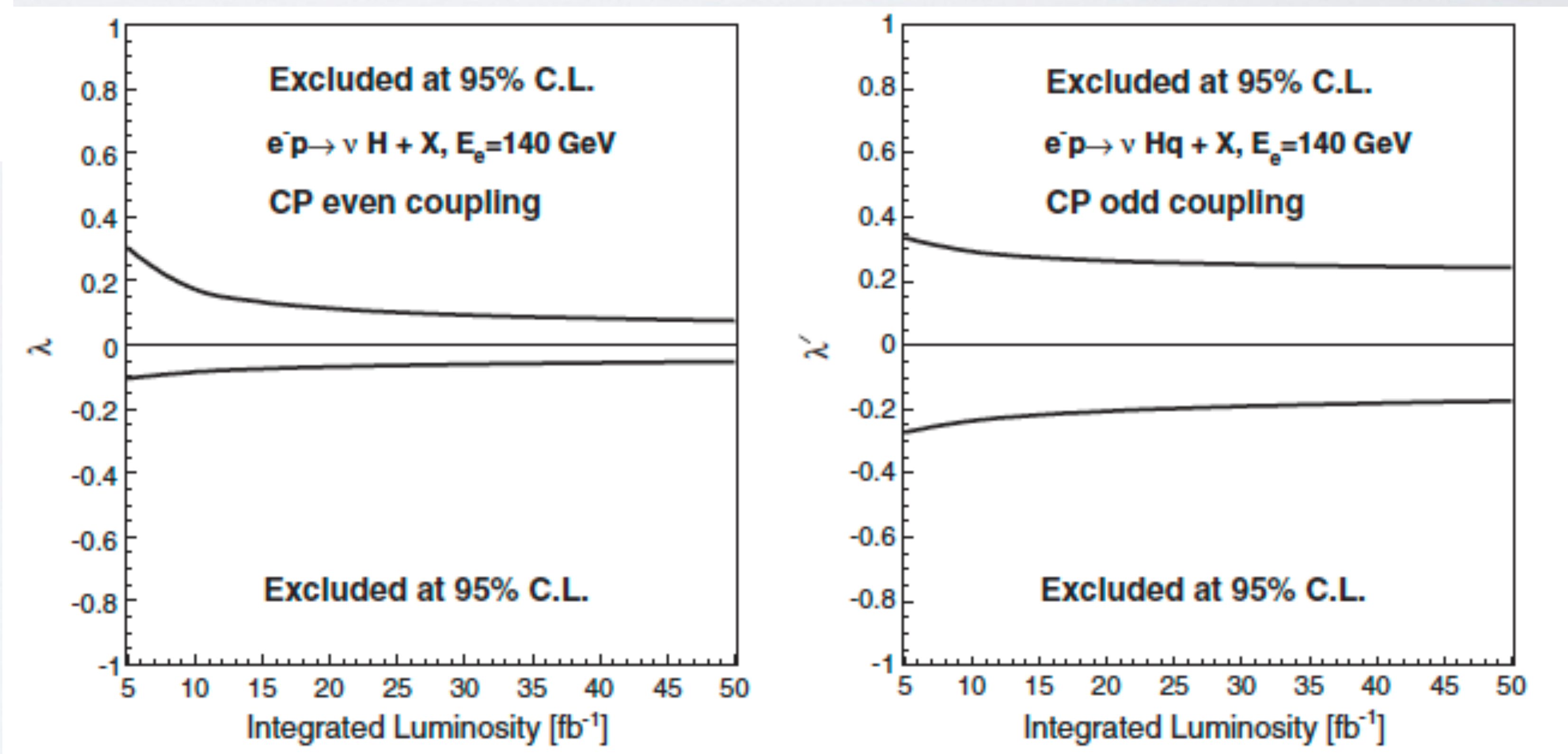

LHeC is the only machine where one can measure the HWW coupling directly without making any prior assumptions about new BSM physics.

II.

Physics Letters B 764 (2017) 247–253

Probing anomalous couplings using di-Higgs production in electron–proton collisions

Mukesh Kumar[a,*], Xifeng Ruan[b], Rashidul Islam[c], Alan S. Cornell[a], Max Klein[d], Uta Klein[d], Bruce Mellado[b]

$$V(\Phi) = \mu^2 \Phi^\dagger \Phi + \lambda(\Phi^\dagger \Phi)^2 \rightarrow \frac{1}{2} m_h^2 h^2 + \lambda v h^3 + \frac{\lambda}{4} h^4, \quad (1)$$

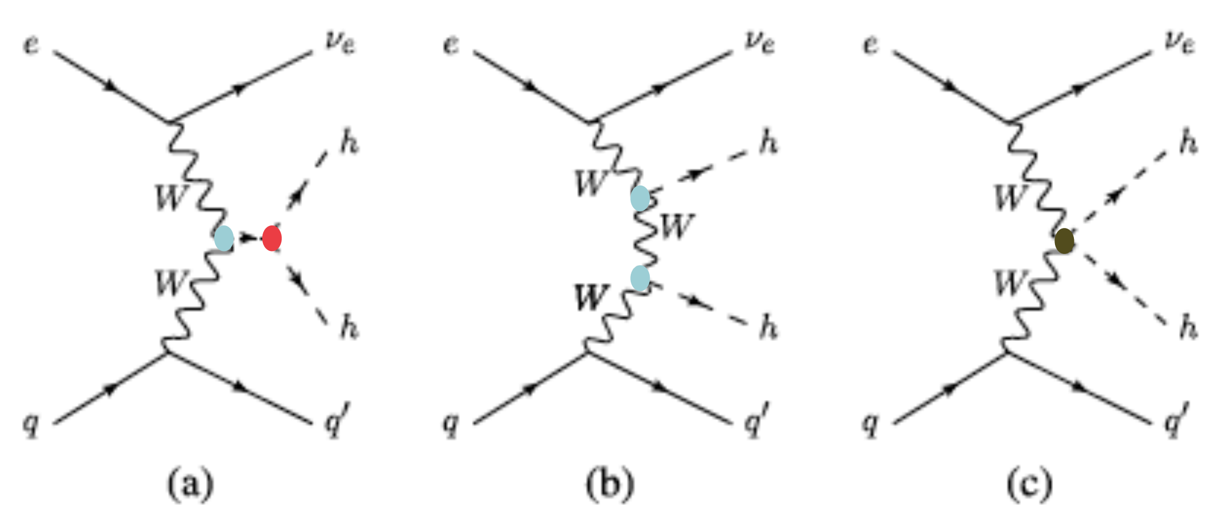

Fig. 1. Leading order diagrams contributing to the process $p e^- \rightarrow hhj\nu_e$ with $q \equiv u, c, \bar{d}, \bar{s}$ and $q' \equiv d, s, \bar{u}, \bar{c}$ respectively.

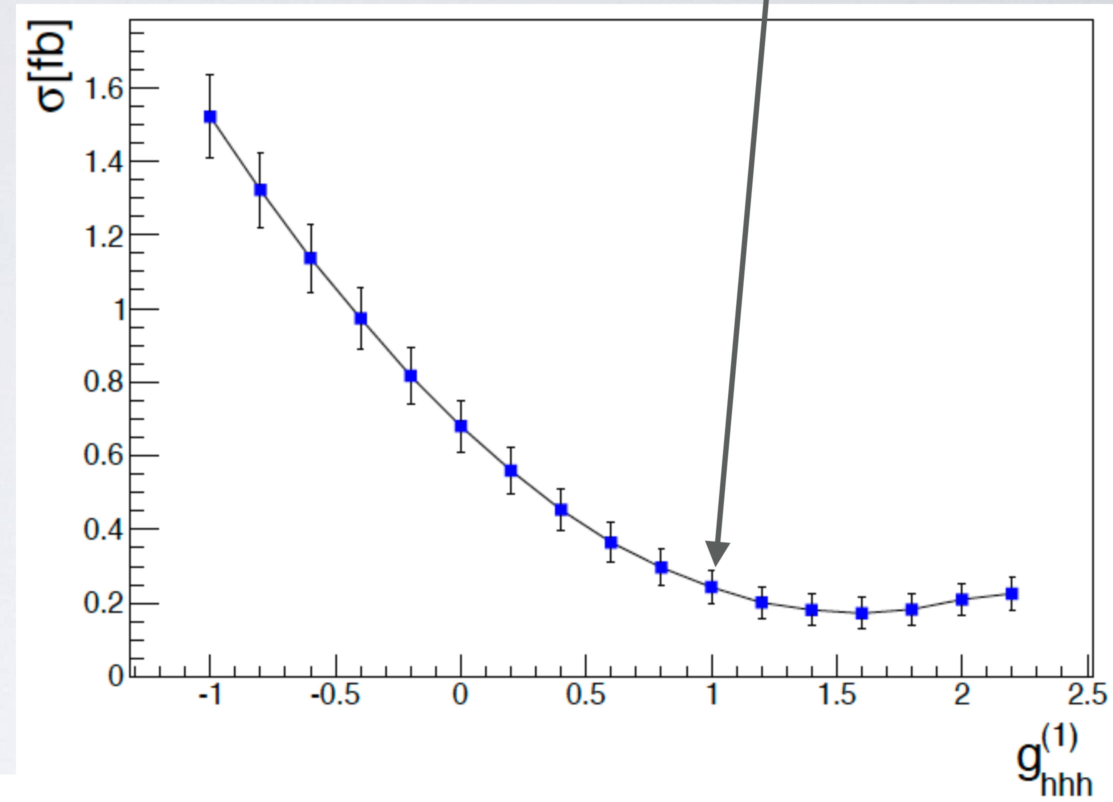

Table 1
Cross sections of signal and backgrounds in charged current (CC), neutral current (NC) and photo-production (PHOTO) modes for $E_e = 60$ GeV and $E_p = 50$ TeV, where j is light quarks and gluons. For this estimation we use basic cuts $|\eta| \leq 10$ for light-jets, leptons and b-tagged jets, $p_T \geq 10$ GeV, $\Delta R_{\min} = 0.4$ for all particles. And electron polarisation is taken to be -0.8.

Process	CC (fb)	NC (fb)	PHOTO (fb)
Signal:	2.40×10^{-1}	3.95×10^{-2}	3.30×10^{-6}
$b\bar{b}b\bar{b}j$:	8.20×10^{-1}	$3.60 \times 10^{+3}$	$2.85 \times 10^{+3}$
$b\bar{b}jjj$:	$6.50 \times 10^{+3}$	$2.50 \times 10^{+4}$	$1.94 \times 10^{+6}$
ZZj ($Z \rightarrow b\bar{b}$):	7.40×10^{-1}	1.65×10^{-2}	1.73×10^{-2}
$t\bar{t}j$ (hadronic):	3.30×10^{-1}	$1.40 \times 10^{+2}$	$3.27 \times 10^{+2}$
$t\bar{t}j$ (semi-leptonic):	1.22×10^{-1}	$4.90 \times 10^{+1}$	$1.05 \times 10^{+2}$
$hb\bar{b}j$ ($h \rightarrow b\bar{b}$):	5.20×10^{-1}	1.40×10^{0}	2.20×10^{-2}
hZj ($Z, h \rightarrow b\bar{b}$):	6.80×10^{-1}	9.83×10^{-3}	6.70×10^{-3}

Signal:

$\mathtt{CC}: p\, e^- \rightarrow \nu_e\, h\, h\, j$

$\mathtt{NC}: p\, e^- \rightarrow e^-\, h\, h\, j$

$\mathtt{PHOTO}: p\, \gamma \rightarrow h\, h\, j$

Backgrounds

Formalism

Effective Field Theory Approach (EFT) derived from dimension less than or equal to six:

[arXiv: 1310.5150]

The complete Lagrangian we work with is as follows:

$$\mathcal{L} = \mathcal{L}_{SM} + \mathcal{L}^{(3)}_{hhh} + \mathcal{L}^{(3)}_{hWW} + \mathcal{L}^{(4)}_{hhWW}. \quad (5)$$

The most general effective vertices take the form:

$$\Gamma_{hhh} = -6\lambda v\left[g^{(1)}_{hhh} + \frac{g^{(2)}_{hhh}}{3m_h^2}(p_1\cdot p_2 + p_2\cdot p_3 + p_3\cdot p_1)\right], \quad (6)$$

$$\Gamma_{hW^-W^+} = g m_W\left[\left\{1 + \frac{g^{(1)}_{hWW}}{m_W^2}p_2\cdot p_3 + \frac{g^{(2)}_{hWW}}{m_W^2}(p_2^2+p_3^2)\right\}\eta^{\mu_2\mu_3} - \frac{g^{(1)}_{hWW}}{m_W^2}p_2^{\mu_3}p_3^{\mu_2} - \frac{g^{(2)}_{hWW}}{m_W^2}(p_2^{\mu_2}p_2^{\mu_3} + p_3^{\mu_2}p_3^{\mu_3}) - i\frac{\tilde{g}_{hWW}}{m_W^2}\epsilon_{\mu_2\mu_3\mu\nu}p_2^{\mu}p_3^{\nu}\right], \quad (7)$$

$$\Gamma_{hhW^-W^+} = g^2\left[\left\{\frac{1}{2} + \frac{g^{(1)}_{hhWW}}{m_W^2}p_3\cdot p_4 + \frac{g^{(2)}_{hhWW}}{m_W^2}(p_3^2+p_4^2)\right\}\eta^{\mu_3\mu_4} - \frac{g^{(1)}_{hhWW}}{m_W^2}p_3^{\mu_4}p_4^{\mu_3} - \frac{g^{(2)}_{hhWW}}{m_W^2}(p_3^{\mu_3}p_3^{\mu_4} + p_4^{\mu_3}p_4^{\mu_4}) - i\frac{\tilde{g}_{hhWW}}{m_W^2}\epsilon_{\mu_3\mu_4\mu\nu}p_3^{\mu}p_4^{\nu}\right]. \quad (8)$$

$$\mathcal{L}^{(3)}_{hhh} = \frac{m_h^2}{2v}(1 - g^{(1)}_{hhh})h^3 + \frac{1}{2v}g^{(2)}_{hhh}h\partial_\mu h\partial^\mu h, \quad (2)$$

$$\mathcal{L}^{(3)}_{hWW} = -g\left[\frac{g^{(1)}_{hWW}}{2m_W}W^{\mu\nu}W^\dagger_{\mu\nu}h + \frac{g^{(2)}_{hWW}}{m_W}(W^\nu\partial^\mu W^\dagger_{\mu\nu}h + \text{h.c}) + \frac{\tilde{g}_{hWW}}{2m_W}W^{\mu\nu}\widetilde{W}^\dagger_{\mu\nu}h\right], \quad (3)$$

$$\mathcal{L}^{(4)}_{hhWW} = -g^2\left[\frac{g^{(1)}_{hhWW}}{4m_W^2}W^{\mu\nu}W^\dagger_{\mu\nu}h^2 + \frac{g^{(2)}_{hhWW}}{2m_W^2}(W^\nu\partial^\mu W^\dagger_{\mu\nu}h^2 + \text{h.c}) + \frac{\tilde{g}_{hhWW}}{4m_W^2}W^{\mu\nu}\widetilde{W}^\dagger_{\mu\nu}h^2\right]. \quad (4)$$

Here:

$$W_{\mu\nu} = \partial_\mu W_\nu - \partial_\nu W_\mu$$

$$\tilde{W}_{\mu\nu} = \frac{1}{2}\epsilon_{\mu\nu\rho\sigma}W^{\rho\sigma}$$

CP Even: $g^{(i)}_{(\ldots)}, i = 1, 2$

CP Odd: $\tilde{g}_{(\ldots)}$

II.

Optimisation of Events

Table 2

A summary table of event selections to optimise the signal with respect to the backgrounds in terms of the weights at 10 ab^{-1}. In the first column the selection criteria are given as described in the text. The second column contains the weights of the signal process $pe^- \to hhj\nu_e$, where both the Higgs bosons decay to $b\bar{b}$ pair. In the next columns the sum of weights of all individual prominent backgrounds in charged current, neutral current and photo-production are given with each selection, whereas in the penultimate column all backgrounds' weights are added. The significance is calculated at each stage of the optimised selection criteria using the formula $\mathcal{S} = \sqrt{2[(S+B)\log(1+S/B) - S]}$, where S and B are the expected signal and background yields at a luminosity of 10 ab^{-1} respectively. This optimisation has been performed for $E_e = 60$ GeV and $E_p = 50$ TeV.

Cuts/Samples	Signal	$4b+$jets	$2b+$jets	Top	ZZ	$b\bar{b}H$	ZH	Total Bkg	Significance
Initial	2.00×10^3	3.21×10^7	2.32×10^9	7.42×10^6	7.70×10^3	1.94×10^4	6.97×10^3	2.36×10^9	0.04
At least $4b + 1j$	3.11×10^2	7.08×10^4	2.56×10^4	9.87×10^3	7.00×10^2	6.32×10^2	7.23×10^2	1.08×10^5	0.94
Lepton rejection $p_T^\ell > 10$ GeV	3.11×10^2	5.95×10^4	9.94×10^3	6.44×10^3	6.92×10^2	2.26×10^2	7.16×10^2	7.75×10^4	1.12
Forward jet $\eta_J > 4.0$	233	13007.30	2151.15	307.67	381.04	46.82	503.22	16397.19	1.82
$\not{E}_T > 40$ GeV	155	963.20	129.38	85.81	342.18	19.11	388.25	1927.93	3.48
$\Delta\phi_{\not{E}_T j} > 0.4$	133	439.79	61.80	63.99	287.10	14.53	337.14	1204.35	3.76
$m_{bb}^1 \in [95, 125]$, $m_{bb}^2 \in [90, 125]$	54.5	28.69	5.89	6.68	5.14	1.42	17.41	65.23	6.04
$m_{4b} > 290$ GeV	49.2	10.98	1.74	2.90	1.39	1.21	11.01	29.23	7.51

(1) At least $4b + 1 -$ light jet with $p_T > 20\,\mathrm{GeV}$,

(2) $|\eta_b| < 5, |\eta_j| < 7$,

(3) $\Delta R = \sqrt{(\Delta\phi)^2 + (\Delta\eta)^2} > 0.7$,

(4) $p_T^{l^\pm} > 10\,\mathrm{GeV}$ are rejected,

(5) $|\eta_J| > 4.0$,

(6) $MET > 40\ \mathrm{GeV}$,

(7) $\Delta\phi_{MET\,j} > 0.4$,

(8) $m_{bb}^1 \in [95, 125], m_{bb}^2 \in [90, 125]$,

(9) $m_{4b} > 290\ \mathrm{GeV}$.

In the selection the b-tagging efficiency is assumed to be 70%, fake rates from c-initiated jets and light jets to the b-jets of 10% and 1% respectively.

Significance calculated using Poisson formula:

$$\mathcal{S} = \sqrt{2[(S+B)\ \log(1+S/B)] - S]}$$

Azimuthal Angle correlations and Asymmetries

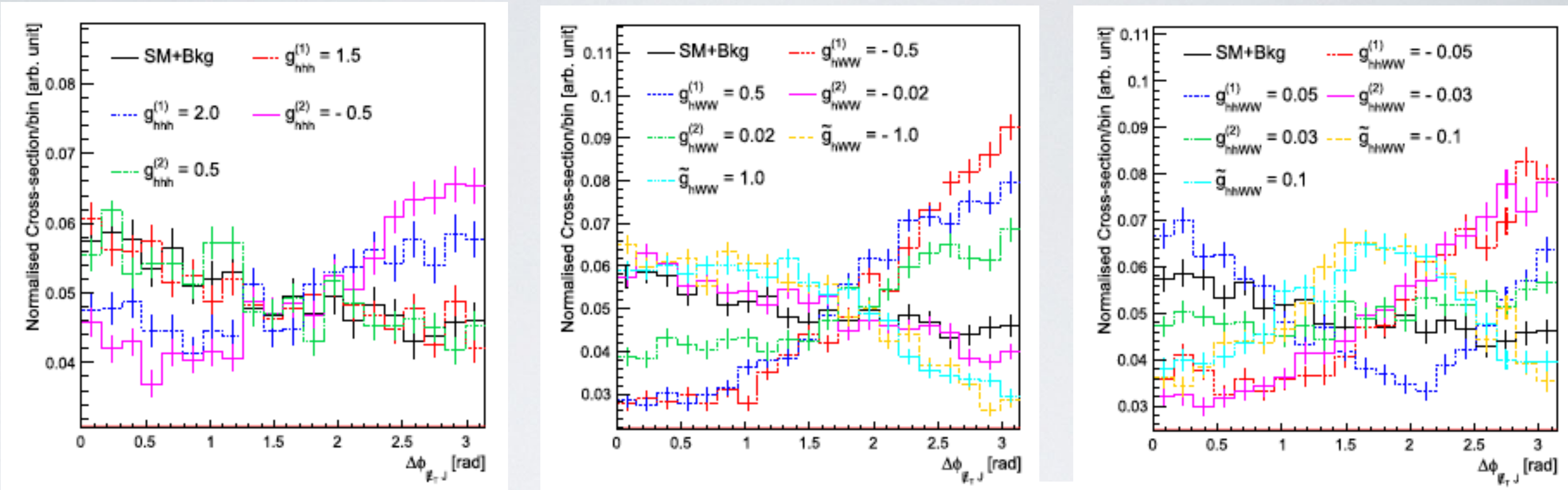

Table 3
Estimation of the asymmetry, defined in Eq. (9), and statistical error associated with the kinematic distributions in Fig. 2 at an integrated luminosity of 10 ab^{-1}. The cross section (σ) for the corresponding coupling choice is given in the last column with same parameters as in Table 1.

Samples		$\mathcal{A}_{\Delta\phi_{\not{E}_T J}}$	σ (fb)
SM+Bkg		0.277 ± 0.088	
$g^{(1)}_{hhh}$	$= 1.5$	0.279 ± 0.052	0.18
	$= 2.0$	0.350 ± 0.053	0.21
$g^{(2)}_{hhh}$	$= -0.5$	0.381 ± 0.050	0.19
	$= 0.5$	0.274 ± 0.024	0.74
$g^{(1)}_{hWW}$	$= -0.5$	0.506 ± 0.022	0.88
	$= 0.5$	0.493 ± 0.020	0.94
$g^{(2)}_{hWW}$	$= -0.02$	0.257 ± 0.025	0.67
	$= 0.02$	0.399 ± 0.040	0.33
$\tilde{g}_{hWW}$	$= -1.0$	0.219 ± 0.016	1.53
	$= 1.0$	0.228 ± 0.016	1.53
$g^{(1)}_{hhWW}$	$= -0.05$	0.450 ± 0.033	0.52
	$= 0.05$	0.254 ± 0.029	0.68
$g^{(2)}_{hhWW}$	$= -0.03$	0.462 ± 0.022	1.22
	$= 0.03$	0.333 ± 0.018	1.46
$\tilde{g}_{hhWW}$	$= -0.1$	0.351 ± 0.020	1.60
	$= 0.1$	0.345 ± 0.020	1.61

Choice of couplings are ad-hoc though these values are derived at 0.4 /ab based on cross sections.
[M. Kumar, J. Phys. Conf. Ser. 645, no. 1, 012005 (2015), arXiv: 1506.03999]

$$\mathcal{A}_{\Delta\phi_{\not{E}_T J}} = \frac{|A_{\Delta\phi>\pi/2}| - |A_{\Delta\phi<\pi/2}|}{|A_{\Delta\phi>\pi/2}| + |A_{\Delta\phi<\pi/2}|}$$

II. Exclusion Limits of couplings at FCC-he: Ee = 60 GeV, Ep = 50 TeV (fiducial cross sections)

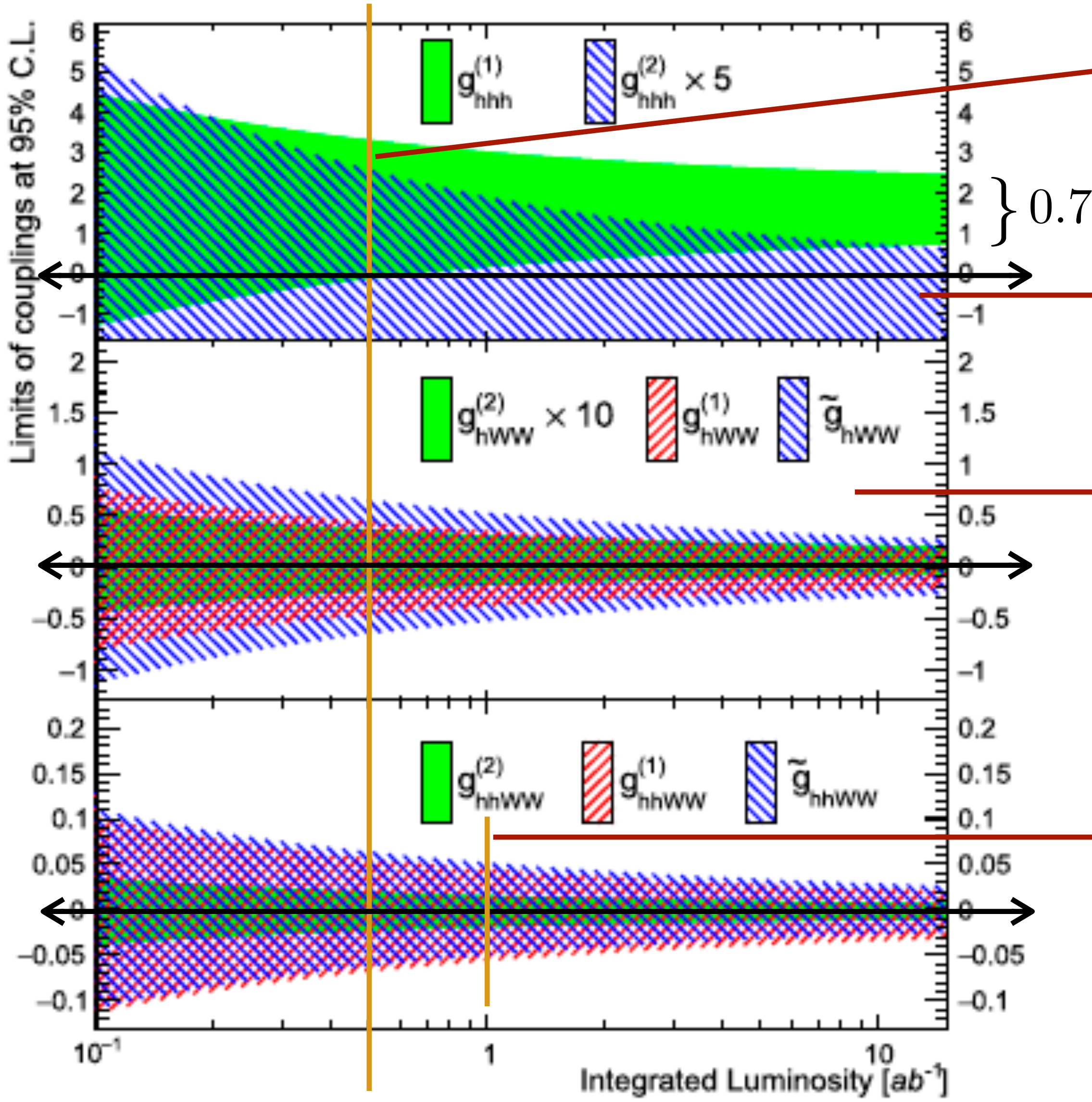

Fig. 3. The exclusion limits on the anomalous hhh (top panel), hWW (middle panel) and $hhWW$ (lower panel) couplings at 95% C.L. as a function of integrated luminosity (shaded areas). Note that the allowed values of $g^{(2)}_{hhh}$ and $g^{(2)}_{hWW}$ are multiplied by 5 and 10 respectively to highlight their exclusion region, since the values are of the order 10^{-1}.

$g^{(1)}_{hhh}$ is positive

$\}\ 0.7 - 2.5$ at 15 ab^{-1}

$g^{(2)}_{hhh}$ is restricted to around 10^{-1}

$g^{(1)}_{hWW}$ and $\tilde{g}_{hWW}$ can better probed at LHeC, while $g^{(2)}_{hWW}$ here is restricted of the order 10^{-2}

constraint on these couplings increases and limits are reduce by a factor of 2

5% Systematics

Using signal injection test, locally measured one-sigma error bound around the expected SM strength of Higgs-self coupling is :

$$g^{(1)}_{hhh} = 1.00^{+0.24(0.14)}_{-0.17(0.12)} \text{ at } \sqrt{s} = 3.5(5.0) \text{ TeV for an ultimate 10 ab}^{-1}$$

II. Degradation of anomalous couplings w.r.t scale of higher dimensional operators:

$$\mathcal{L} = \mathcal{L}_{\rm SM} + \frac{1}{\Lambda}\mathcal{O}^5 + \frac{1}{\Lambda^2}\mathcal{O}^6 + \ldots \quad \Longrightarrow \quad \Sigma \equiv \Sigma(p_i, \Lambda_i, \ldots)$$

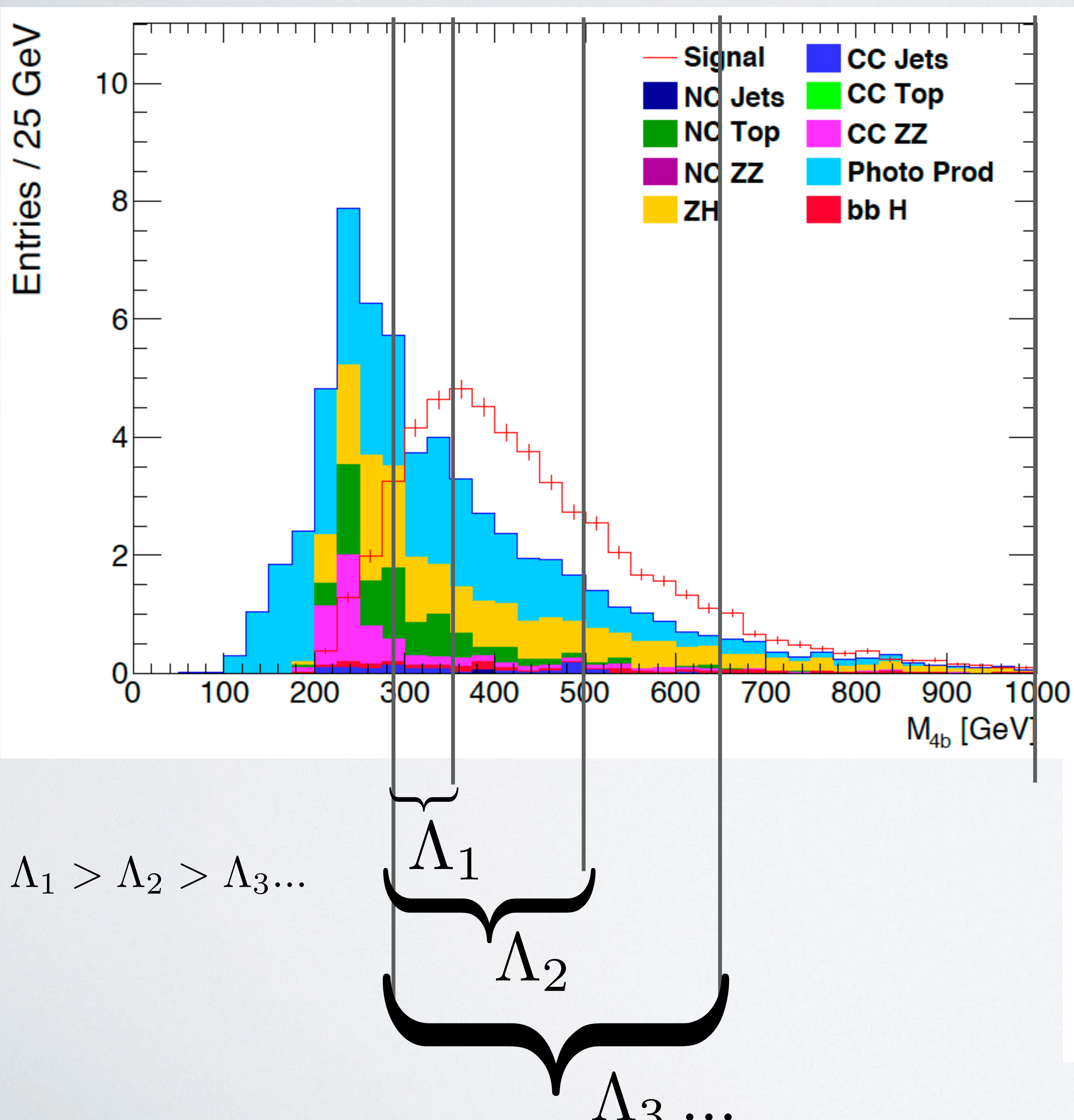

$\Lambda_1 > \Lambda_2 > \Lambda_3 \ldots$

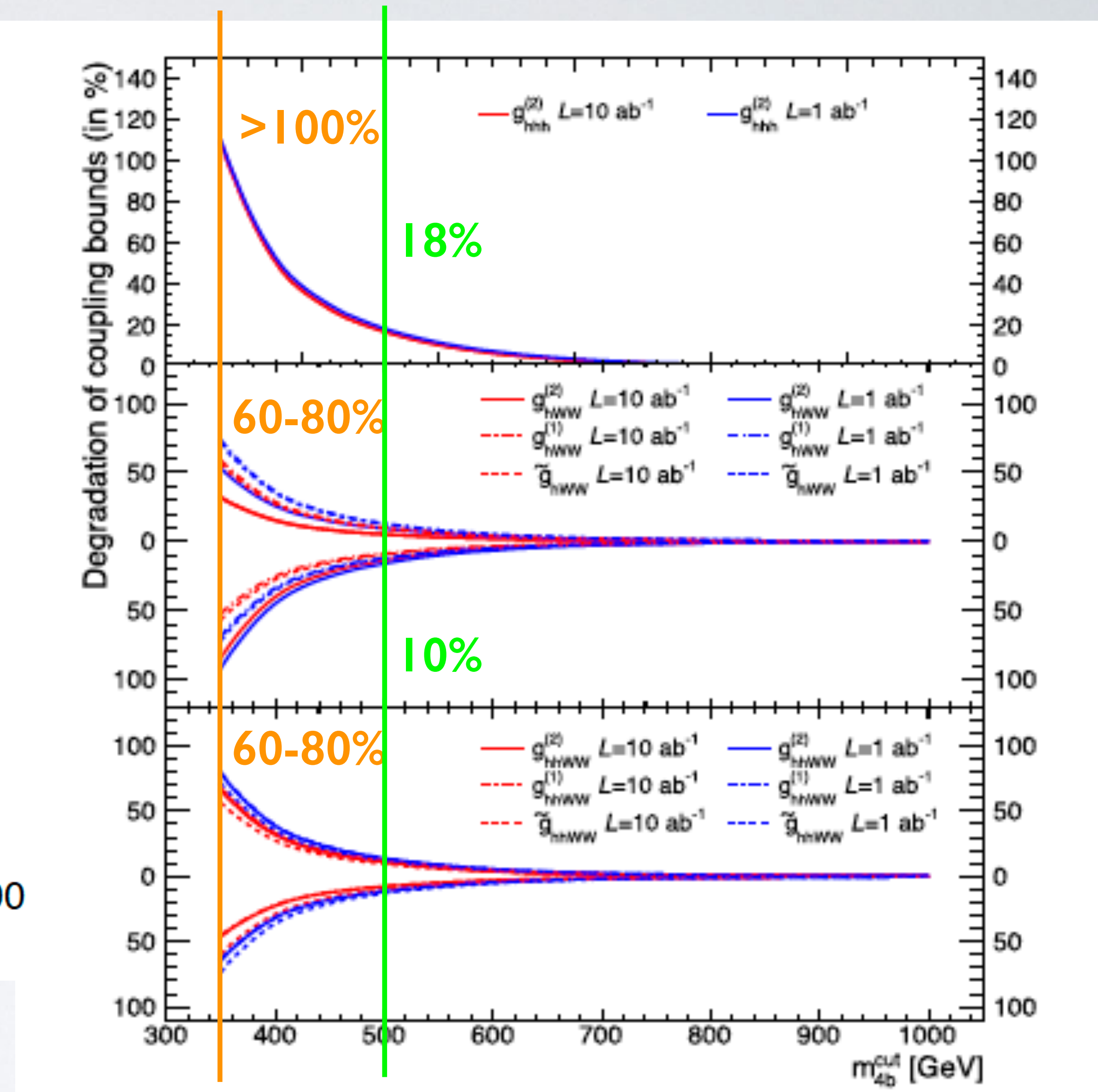

Fig. 4. Percentage of deterioration of exclusion limits of anomalous tensorial couplings (shown in Fig. 3) with respect to the upper di-Higgs invariant mass cut $m'_{4b} \equiv m_{4b}^{\rm cut}$ [in GeV] for fixed luminosity of 1 ab^{-1} (*blue*) and 10 ab^{-1} (*red*). The numbers in the vertical axis above (below) 0 is the degradation in the upper (lower) limits. (For interpretation of the references to colour in this figure legend, the reader is referred to the web version of this article.)

III. One loop electroweak correction to hVV vertices - only Higgs self coupling

Tree level single Higgs-boson production (charged-current) at e-p collider

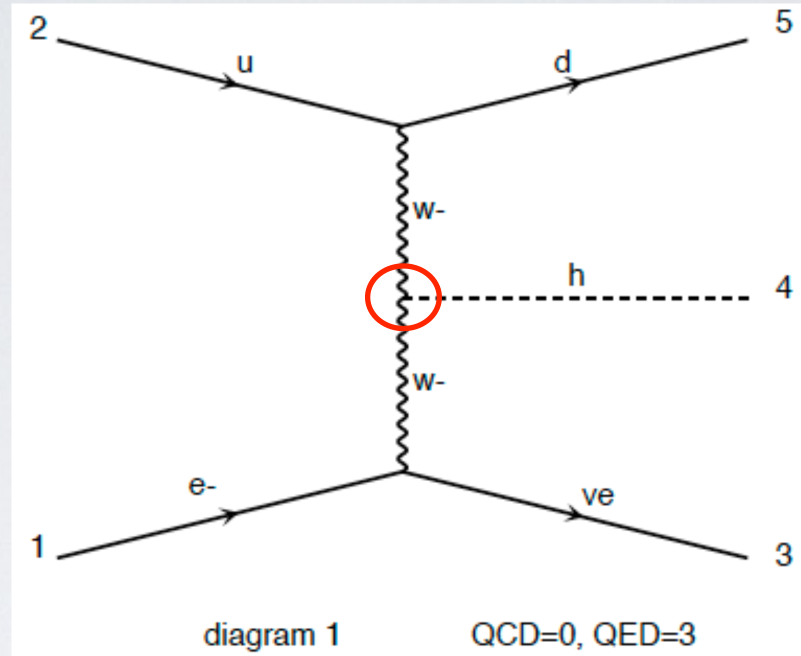

Other production modes include from neutral-current as well as with single anti-top quark in charged-current.

Next to leading order one-loop correction of the order of **Higgs-self coupling** $g_{hhh}^{(1)}$

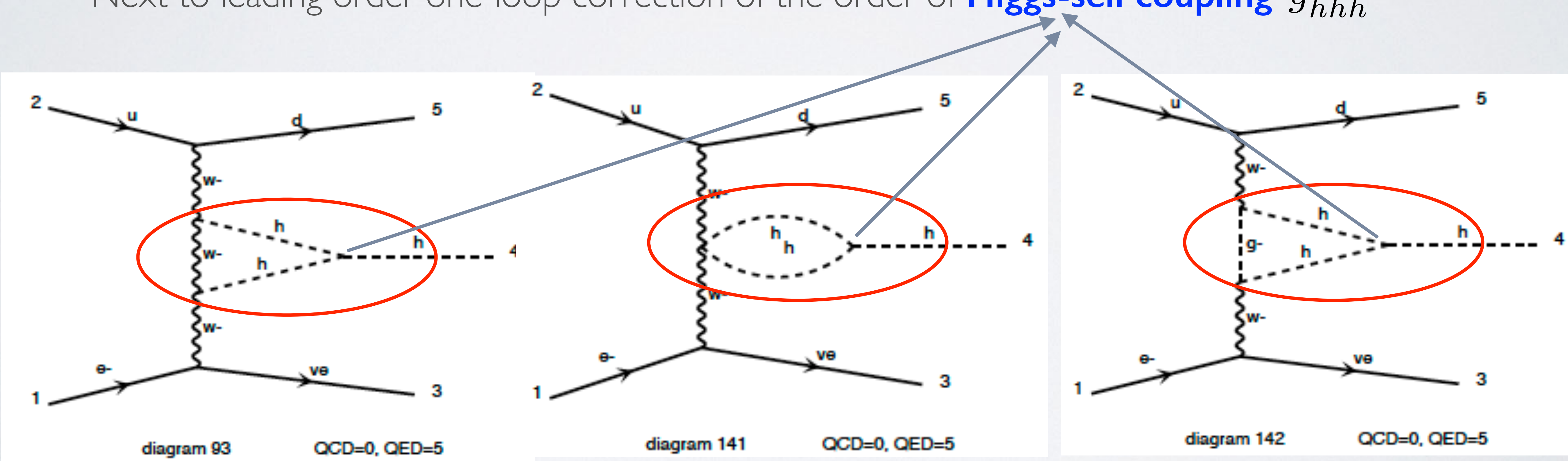

III. **Formalism** based on [JHEP12 (2016) 080, arXiv: 1607.04251]

https://cp3.irmp.ucl.ac.be/projects/madgraph/wiki/HiggsSelfCoupling

$$V(H) = \frac{m_H^2}{2}H^2 + \lambda_3 v H^3 + \lambda_4 H^4 \qquad (m_H^2 = 2\lambda v^2, \lambda_3^{SM} = \lambda, \lambda_4^{SM} = \lambda/4)$$

$$V_{H^3} = \lambda_3 \, v \, H^3 \equiv \kappa_\lambda \lambda_3^{SM} \, v \, H^3, \qquad \lambda_3^{SM} = \frac{G_\mu}{\sqrt{2}} m_H^2, \qquad v = (\sqrt{2} G_\mu)^{-1/2}$$

Denoting as $\mathcal{M}$ a generic amplitude for single Higgs production or a Higgs decay width, the correction to $\mathcal{M}$ induced by the λ_3-dependent diagram of figure 1 can be written as

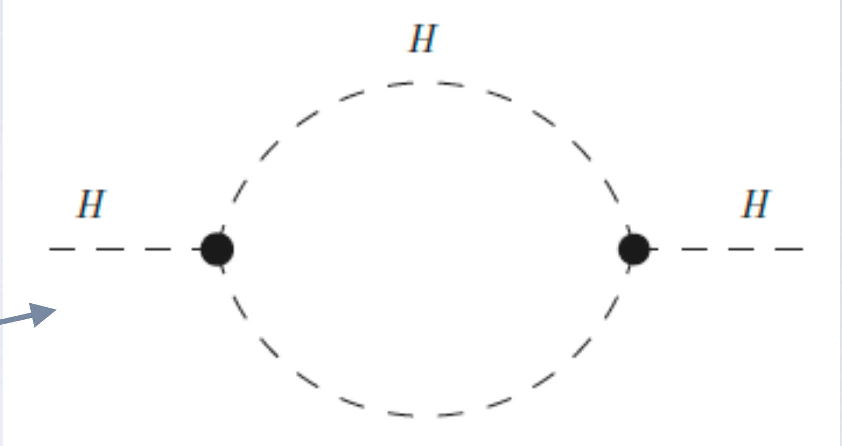

One-loop λ_3-dependent diagram in the Higgs self-energy.

$$(\delta\mathcal{M})_{Z_H} = \left(\sqrt{Z_H} - 1\right)\mathcal{M}^0, \qquad Z_H = \frac{1}{1 - \kappa_\lambda^2 \, \delta Z_H},$$

$$\delta Z_H = -\frac{9}{16}\frac{G_\mu m_H^2}{\sqrt{2}\,\pi^2}\left(\frac{2\pi}{3\sqrt{3}} - 1\right)$$

Note: $\kappa_\lambda \equiv g_{hhh}^{(1)}$

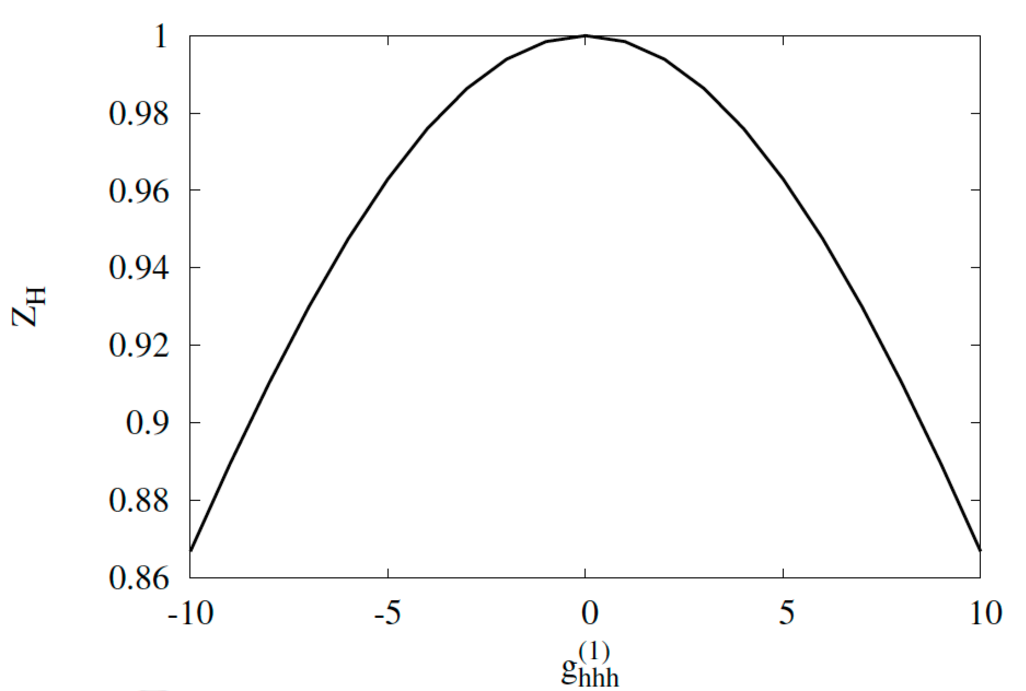

Once all the contributions from $\mathcal{M}^1_{\lambda_3}$ and Z_H are taken into account, denoting as Σ a generic cross section for single Higgs production or a Higgs decay width, the corrections induced by an anomalous trilinear coupling modify the LO prediction (Σ_{LO}) according to

$$\Sigma_{NLO} = Z_H \, \Sigma_{LO} \, (1 + \kappa_\lambda C_1)$$

$$C_1 = \frac{\sigma_{\lambda_3}}{\sigma_{LO}}$$

where the coefficient C_1, which originates from $\mathcal{M}^1_{\lambda_3^{SM}}$, depends on the process and the kinematical observable considered, while Z_H is universal

III. C_1

E_e (GeV)	E_p (TeV)	CC	NC	th
60	7	0.62	0.68	0.69
120	7	0.62	0.68	0.74
60	50	0.60	0.66	0.70

C_1^σ [%]	ggF	VBF	WH	ZH	$t\bar{t}H$
7 TeV	0.66	0.65	1.06	1.23	3.87
8 TeV	0.66	0.65	1.05	1.22	3.78
13 TeV	0.66	0.64	1.03	1.19	3.51
14 TeV	0.66	0.64	1.03	1.18	3.47

LHC

Observables:

Cross section

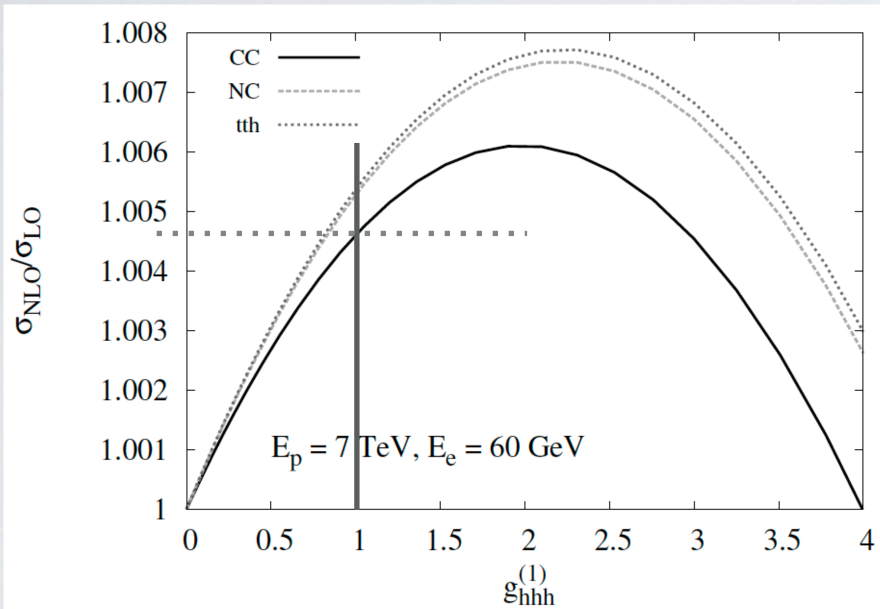

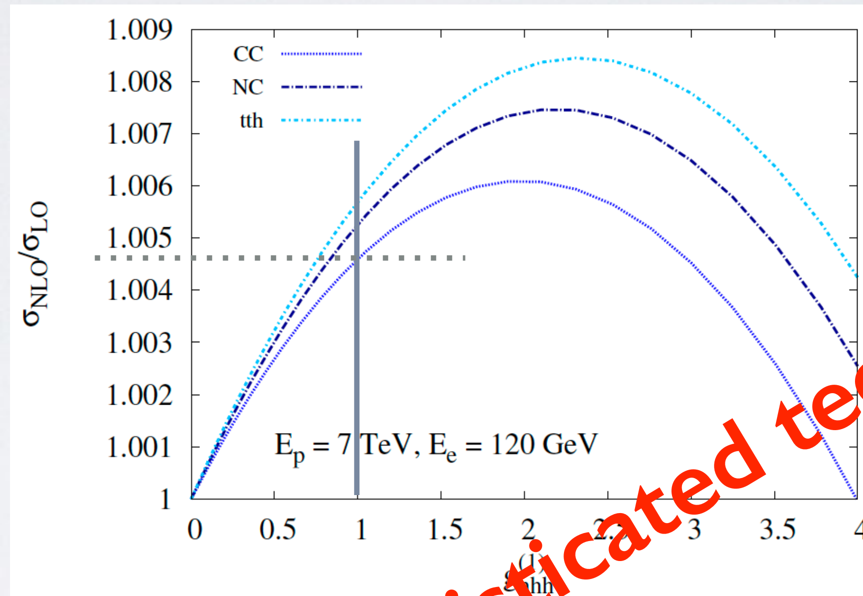

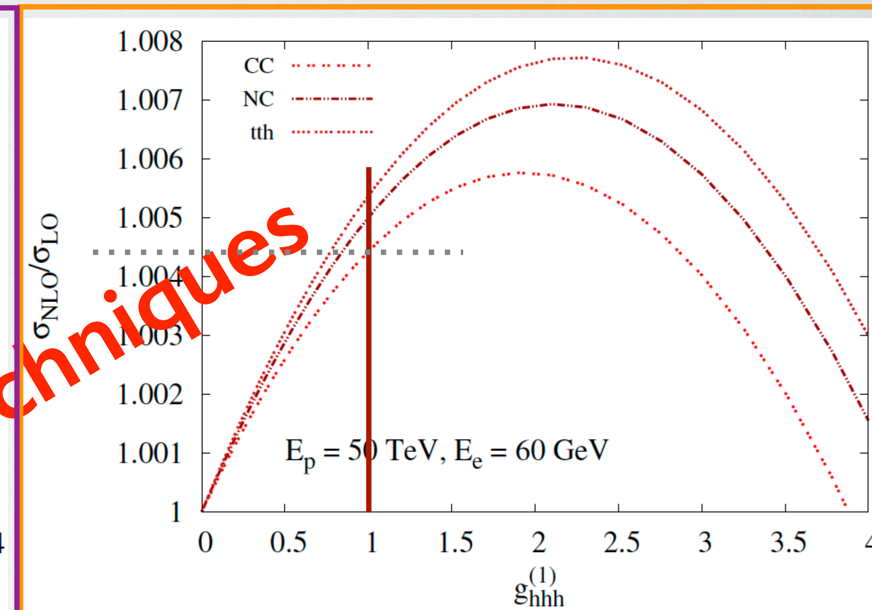

Needs more sophisticated techniques

Transverse momentum p_T

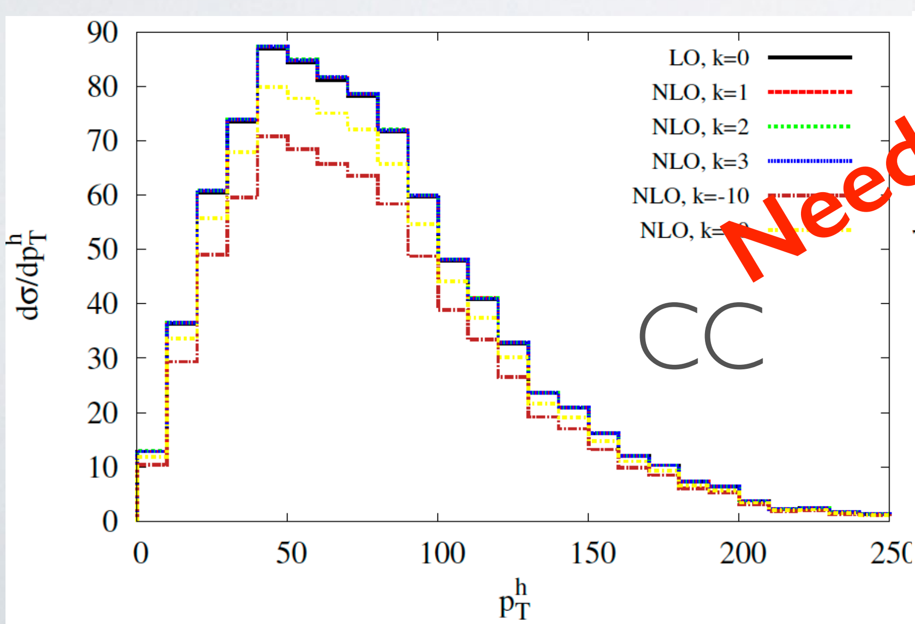

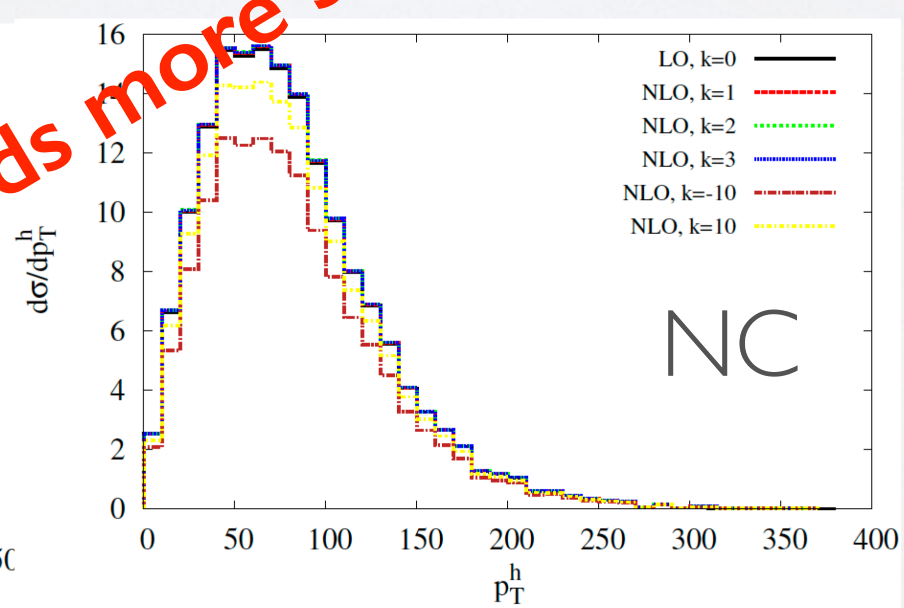

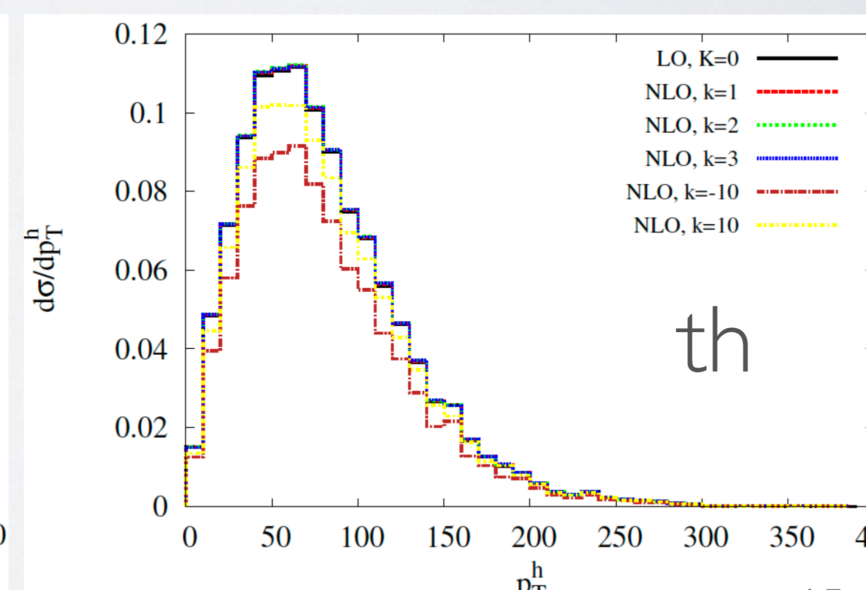

IV.

Exploring CP-even scalars of a Two Higgs-doublet model in future e-p colliders

[M. Kumar et.al, arXiv: 1707.05997]

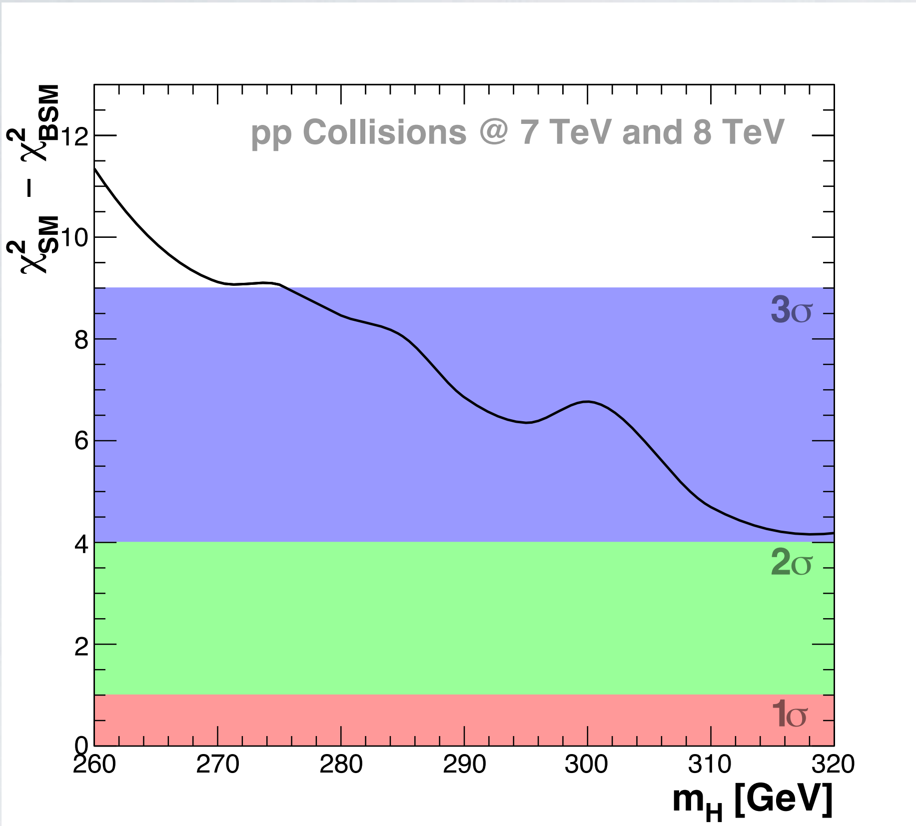

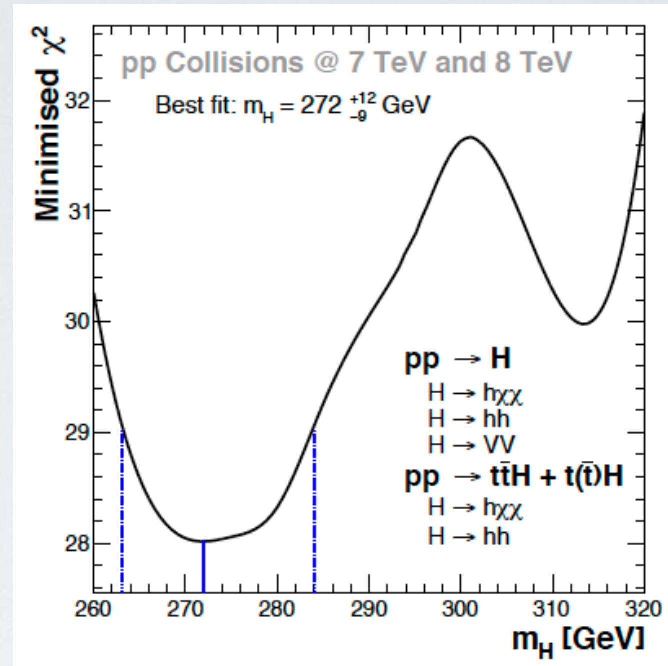

[ArXiv:1506.00612,1603.01208, 1606.01674,1608.03466]

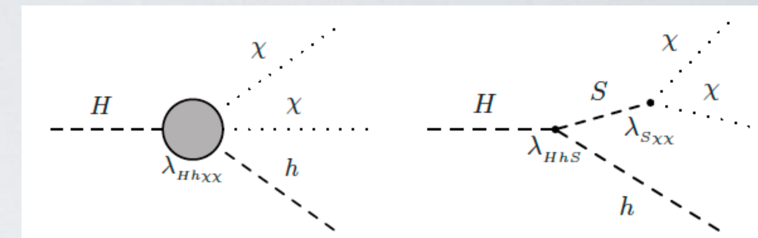

Best Fit results:

$$m_H = 272^{+12}_{-9}\ \text{GeV}$$

3.6σ around 240-250 GeV

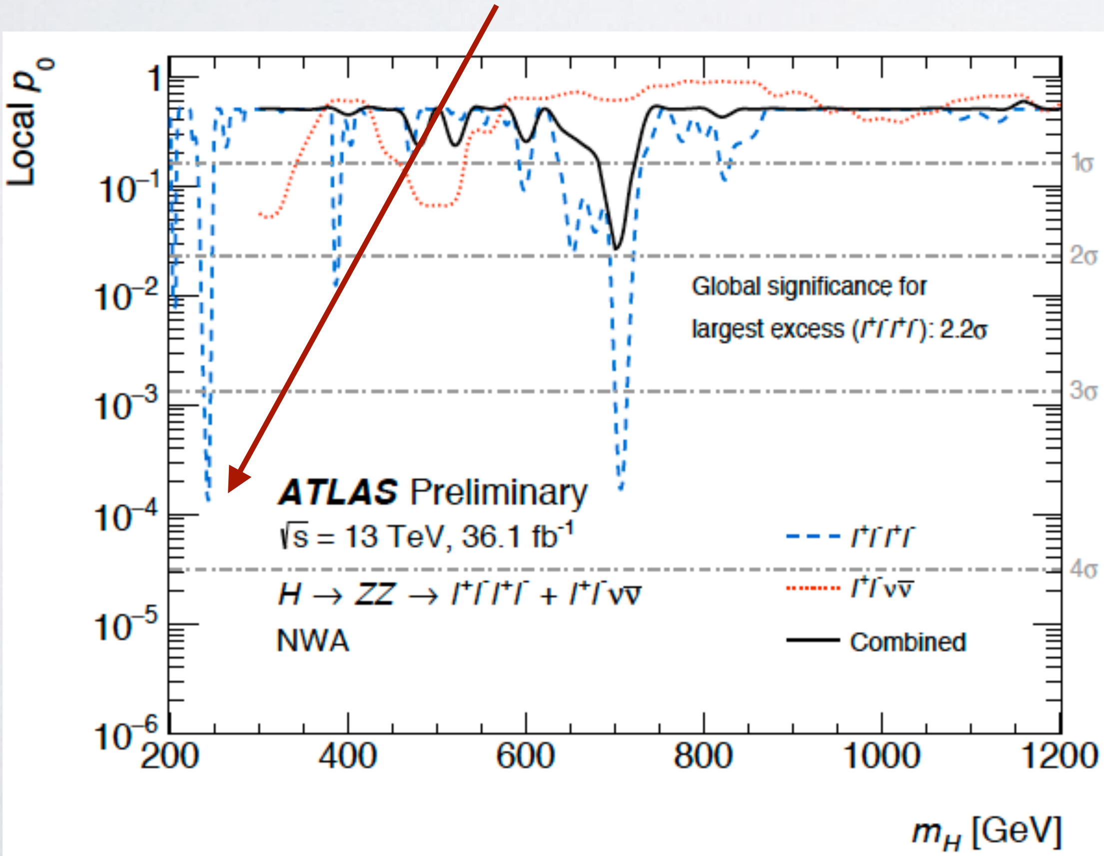

~260-270 GeV

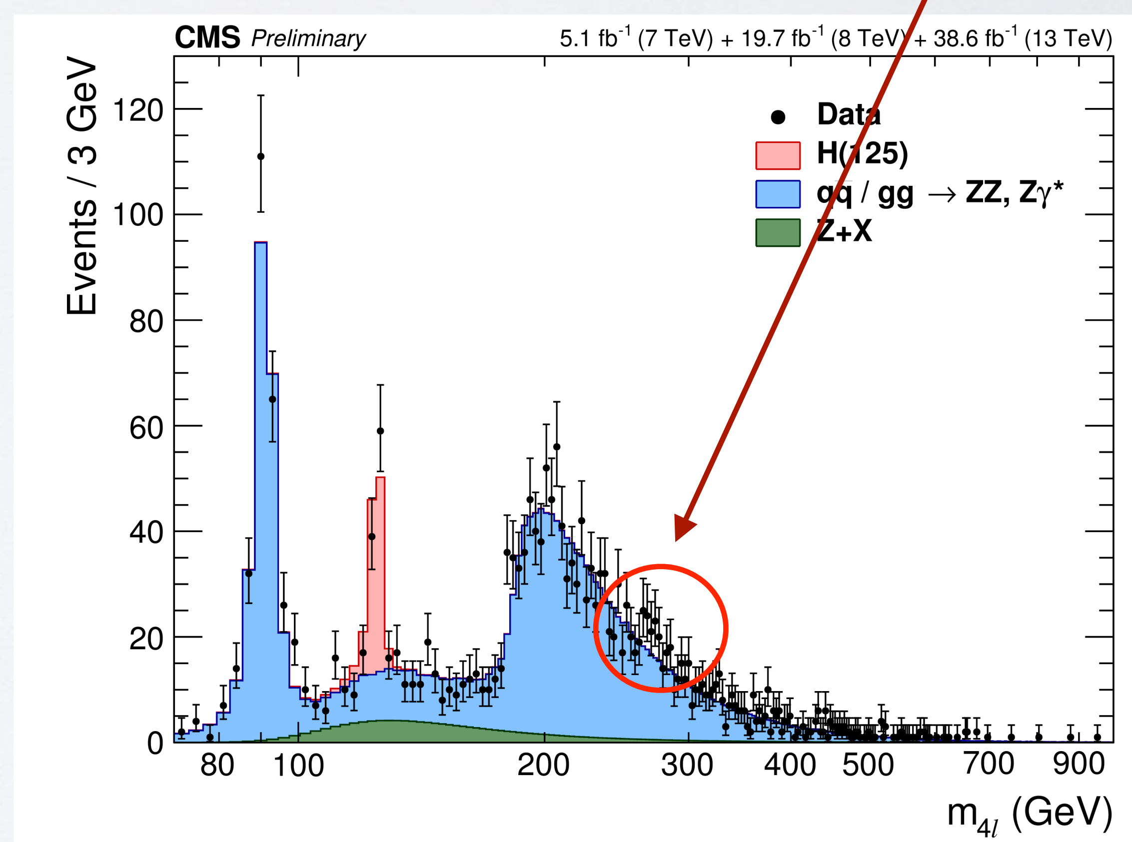

IV.

[M. Kumar et.al, arXiv: 1707.05997]

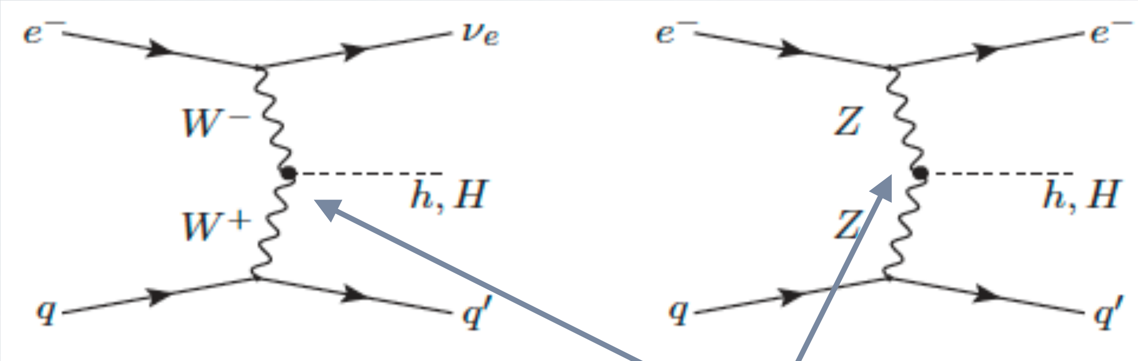

$\propto \sin(\beta-\alpha), \cos(\beta-\alpha)$

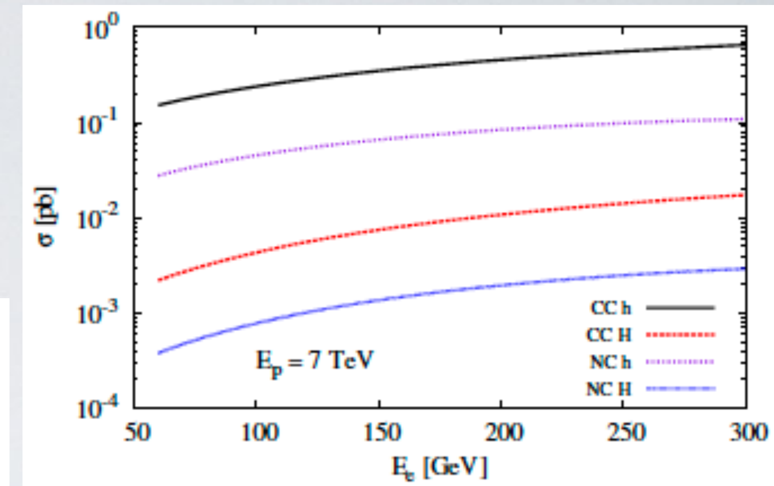

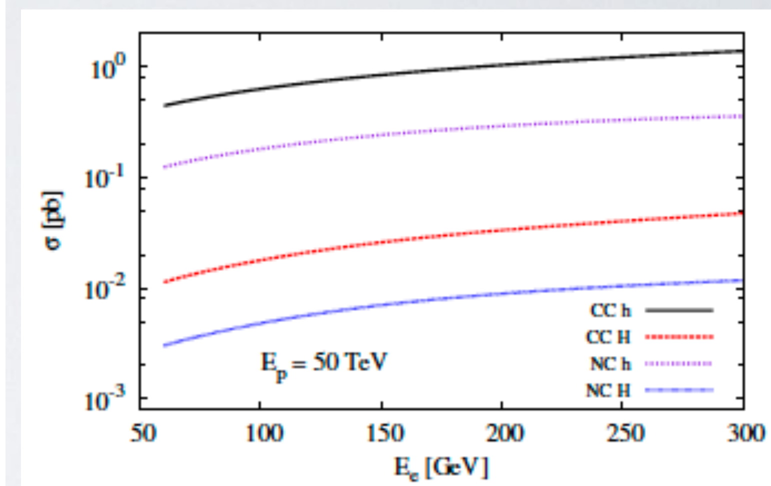

Table 2. Branching ratio of h, H, A and $H^\pm$ by considering the parameter choices as: $m_h = 125$ GeV, $m_H = 270$ GeV, $m_A = 450$ GeV and $m_{H^\pm} = 400$ GeV, $\tan\beta = 1$, $\alpha = -0.53$, $\lambda_1 = 0.1$, $\lambda_2 = 0.27$, $\lambda_3 = 1.1$, $\lambda_4 = -0.5$ and $\lambda_5 = 0.5$ for THDM Type-I. (Dominant BRs are shown in bold)

Modes	h	Modes	H	Modes	A	Modes	$H^\pm$
$b\bar{b}$	**6.5×10^{-1}**	$b\bar{b}$	6.8×10^{-4}	$b\bar{b}$	2.7×10^{-4}	bc	5.9×10^{-7}
$\tau^+\tau^-$	**7.0×10^{-2}**	$\tau^+\tau^-$	8.5×10^{-5}	$\tau^+\tau^-$	3.8×10^{-5}	$\tau\nu$	4.6×10^{-5}
$\mu^+\mu^-$	2.5×10^{-4}	$\mu^+\mu^-$	3.0×10^{-7}	$\mu^+\mu^-$	1.3×10^{-7}	$\mu\nu$	1.6×10^{-7}
$s\bar{s}$	2.5×10^{-4}	$s\bar{s}$	2.6×10^{-7}	$s\bar{s}$	9.6×10^{-8}	su	6.2×10^{-9}
$c\bar{c}$	**3.2×10^{-2}**	$c\bar{c}$	3.3×10^{-5}	$c\bar{c}$	1.4×10^{-5}	cs	1.5×10^{-5}
$t\bar{t}$	0.0×10^{-0}	$t\bar{t}$	8.5×10^{-7}	**$t\bar{t}$**	**7.6×10^{-1}**	**tb**	**8.7×10^{-1}**
gg	**8.5×10^{-2}**	gg	5.5×10^{-4}	gg	3.1×10^{-3}	cd	8.2×10^{-7}
$\gamma\gamma$	1.4×10^{-3}	$\gamma\gamma$	6.7×10^{-6}	$\gamma\gamma$	9.4×10^{-6}	bu	4.1×10^{-9}
$Z\gamma$	1.0×10^{-3}	$Z\gamma$	1.1×10^{-5}	$Z\gamma$	2.4×10^{-6}	ts	1.4×10^{-3}
W^+W^-	**1.4×10^{-1}**	**W^+W^-**	**7.1×10^{-2}**	**Zh**	**5.1×10^{-2}**	td	6.5×10^{-5}
ZZ	**1.8×10^{-2}**	**ZZ**	**3.1×10^{-2}**	**ZH**	**1.84×10^{-1}**	**$hW^\pm$**	**4.6×10^{-2}**
		hh	**9.0×10^{-1}**	W^+H^-	3.6×10^{-5}	**$HW^\pm$**	**8.3×10^{-2}**

Signal:

$H \to hh \to b\bar{b}b\bar{b}$

Signal rate **~ 55%** of total production cross section of **H.** And **dominant background bbbbj at LHeC (FCC-he) - ~2.0 fb (3 times) in CC, ~22 fb (7.5 times) in NC**

!!

Investigating CP nature of $h\tau^+\tau^-$ coupling at the LHeC/FCC-he [Kumar et. al. Wits. Univ.]

Preliminary studies

$$\mathcal{L} \supset -m_\tau \bar{\tau}\tau + \frac{y_t}{\sqrt{2}} \bar{\tau}\left[\cos\zeta_\tau + i\gamma_5 \sin\zeta_\tau\right]\tau\, h,$$

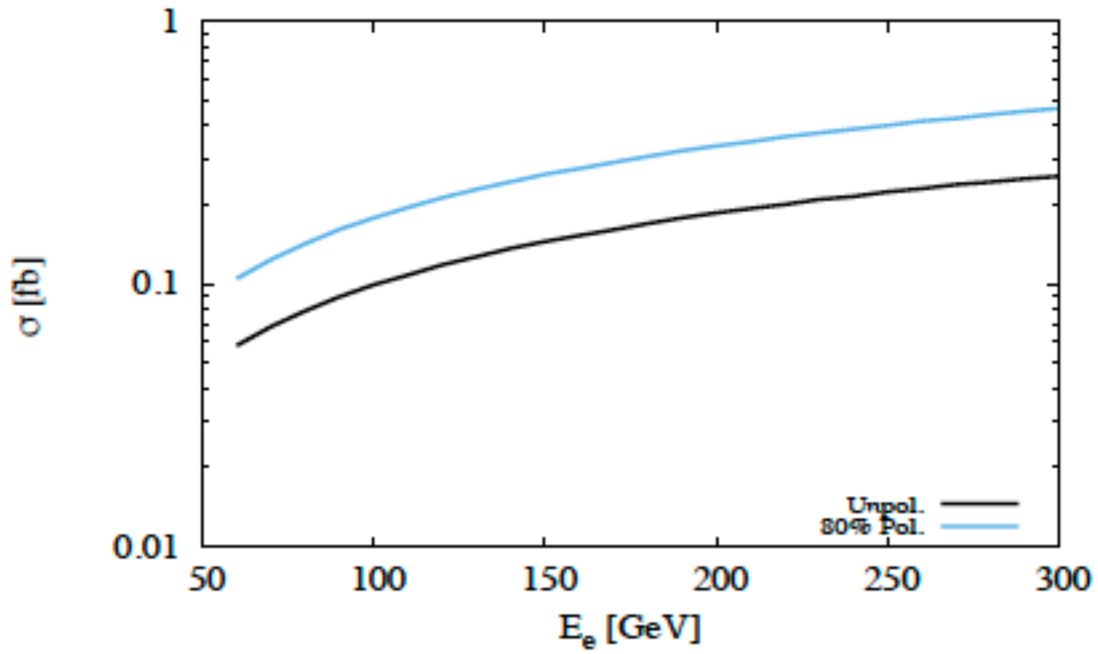

Figure 2: The total cross section against electron beam energy with and without polarization, while the proton beam energy is fixed at 7 TeV. The black solid and dotted dark black lines correspond to the process $p\,e^- \to \nu_e\, h\, j, h \to \tau^+\tau^-(\tau+ \to \pi^+\nu_\tau, \tau- \to \pi^-\bar{\nu}_\tau)$ with and without polarisation of electron beam respectively.

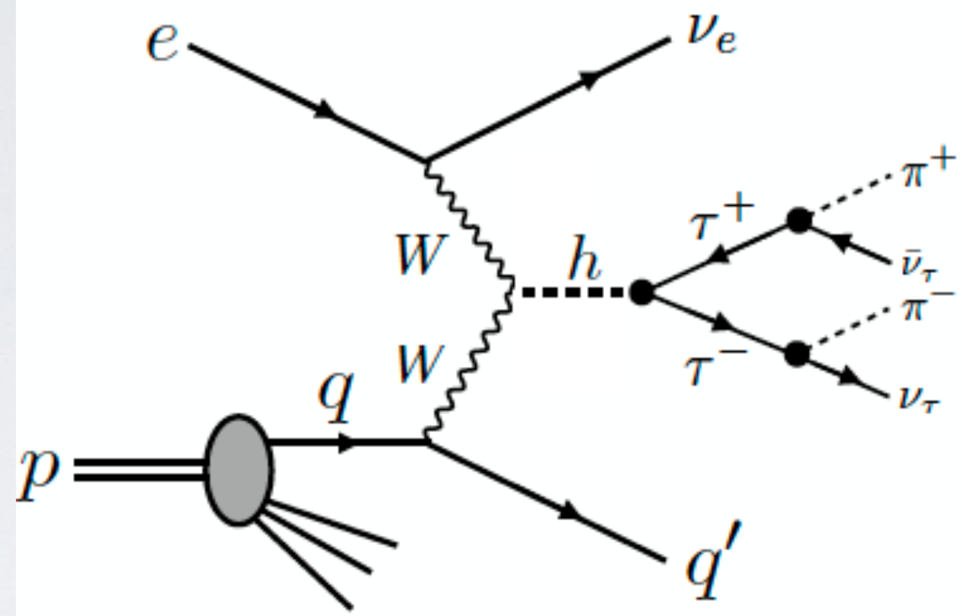

$$\Gamma^{\rm BSM}_{\mu\nu}(p,q) = \frac{g}{M_W}\left[\lambda(p\cdot q\, g_{\mu\nu} - p_\nu q_\mu) + i\lambda' \epsilon_{\mu\nu\rho\sigma} p^\rho q^\sigma\right],$$

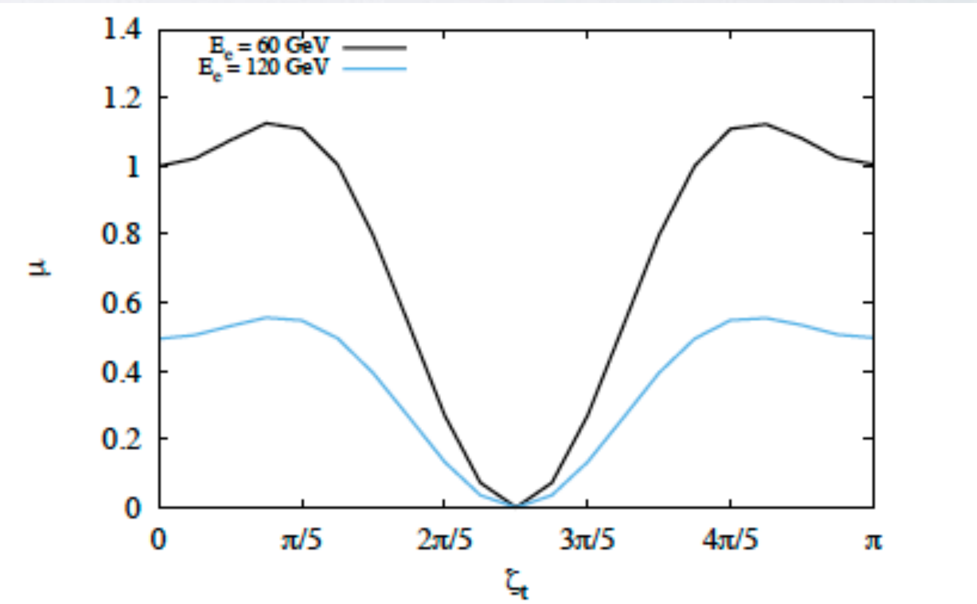

Figure 3: *The signal strength (μ) against CP phase (ζ_τ), the black solid and dotted lines correspond to the electron beam energies of 60 GeV and 120 GeV respectively, while the proton beam energy is fixed at 7 TeV.*

V.

Summary and Discussions:

- An overview of single Higgs production at the LHeC was discussed with hVV EFT couplings to investigate the possibilities of CP-nature of Higgs-boson.
- Double Higgs production opens a very crucial opportunity to study the Higgs-self-coupling and results at FCC-he energies are encouraging (comparatively). An EFT approach also applied to get the limit on other involved couplings like hWW and hhWW.
- Higgs-self coupling can also be probed by Higher Order one-loop electroweak correction to hWW and hZZ vertices - but at both energies of LHeC and FCC-he, measurements of different differential observables are insensitive though the % contribution are similar as LHC. (We note that cross section is sensitive more on FCC-he energies but we need sophisticated techniques to probe more.)
- Based on several features in data from LHC, we suggested mass of CP-even heavy neutral Higgs-boson around 270 GeV and considering that Higgs-boson in a two-Higgs doublet model we investigated the possibilities of rates and dominant modes based on a parameter choices. Further investigation are under study.
- Also Higgs couplings with tau-leptons are under study - which shows how this coupling will be measured at the e-p environment.
- Overall prospects of Higgs-like scalars at the e-p machine are encouraging not only for its production but measuring its couplings with other bosons or fermions in a clean environment.